Scientific Reports

https://doi.org/10.1038/s41598-026-44921-7

Article in Press

Bang-bang control optimization in infectious disease model with incorporating breakthrough and reinfection

Received: 11 December 2025

Accepted: 16 March 2026

Published online: 31 March 2026

Cite this article as: Chen Y., Jing W., Zhang J. *et al.* Bang-bang control optimization in infectious disease model with incorporating breakthrough and reinfection. *Sci Rep* (2026). https://doi.org/10.1038/s41598-026-44921-7

Ya Chen, Wenjun Jing, Juping Zhang & Peng Qin

Bang-Bang Control Optimization in Infectious Disease Model with Incorporating Breakthrough and Reinfection

Ya Chen[1], Wenjun Jing[2,3], Juping Zhang[3,4,5], Peng Qin[6]

[1]*School of Mathematics, Xi'an University of Finance and Economics, Xi'an, Shaanxi 710100, China*

[2]*School of Statistics, Shanxi University of Finance and Economics, Taiyuan, Shanxi, 030006, China*

[3]*Complex Systems Research Center, Shanxi University, Taiyuan, Shanxi 030006, China*

[4]*Shanxi Key Laboratory for Mathematical Technology in Complex Systems, Shanxi University, Taiyuan Shanxi, 030006, China*

[5]*Key Laboratory of Complex Systems and Data Science of Ministry of Education, Shanxi University, Taiyuan Shanxi, 030006, China*

[6]*School of Electrical and Control Engineering, North University of China, Taiyuan Shanxi, 030006, China*

Abstract: Breakthrough infections and reinfection are key factors leading to recurrent epidemic waves. However, sustained control strategies can lead to unnecessary resource wastage when tacking these issues. There is an urgent need to establish dynamic intervention systems capable of rapid response and efficient resource utilization. To address the question of how breakthrough infections and reinfections affect the dynamics of the pandemic, this study develops an infectious disease model that incorporates both breakthrough infections and reinfections, and while introduces bang-bang optimal control as an efficient public health intervention strategy to provide a new perspective and solutions. In theoretical analysis, we derive basic reproduction number via next-generation matrix method, prove the global stability of the disease-free equilibrium, and establish sufficient conditions for the existence of multiple endemic equilibria and the occurrence of backward bifurcation. Numerical simulations further confirm the critical role of breakthrough infections and reinfection in disease persistence and recurrent outbreaks. In control strategy research, we prove the existence of bang-bang optimal solutions based on optimal control theory and demonstrate their distinct advantages in rapidly outbreaks while minimizing operational costs. Simulation results show that a combined strategy implemented under the bang-bang control —reducing transmission rates, expanding vaccine

[6]Corresponding author: qinpeng@nuc.edu.cn

coverage, and enhancing vaccine protection—most effectively contains disease spread. This results provide both theoretical foundation and practical guidance for developing efficient control strategies against recurrent infectious disease outbreaks.

Keywords: Breakthrough Infection; Reinfection; Basic Reproduction Number ; Backward Bifurcations; Bang-Bang Control.

1 Introduction

Breakthrough infection refers to the occurrence of infection by the corresponding pathogen after vaccination, indicating that the vaccine fails to confer complete immunity to the recipient [1]. Breakthrough infection is closely related to various immune response states such as immune failure, immune ineffectiveness, and immune decay [2]. Its occurrence is affected by multiple factors, including vaccine efficacy, the recipient's own immunity, viral antigen variation, and individual differences. The occurrence of breakthrough infection makes it difficult for the vaccine protection rate to reach 100% [3]. Currently, vaccines for SARS-Cov-2, influenza, chickenpox, mumps and other viruses can lead to breakthrough infections [4–6]. Usually, the symptoms of breakthrough infection are milder than those of ordinary infection, and even asymptomatic infection may occur [7, 8].

Reinfection refers to a subsequent infection with the same virus or after recovery [9, 10] For example, COVID-19, influenza, HIV/AIDS, malaria, dengue fever, and other diseases all carry a risk of reinfection [11–15] . Many people who have experienced multiple COVID-19 infections experience milder symptoms due to immunity from prior infections. Though exceptions exist primarily immunocompromised individuals, the elderly, or those with a history of severe infection [16]. Many people who had a severe first infection may be hospitalized or need to go to the hospital again because of reinfection [17]. For example, people living with HIV have a higher rate of reinfection than those without HIV [18, 19].

Breakthrough infections and reinfection are key factors driving disease recurrence, as evidenced by the large-scale COVID-19 waves observed from late 2021 to 2022. As the virus continues to evolve, the emergence of novel variants capable of evading existing immunity may further increase the risks of breakthrough infection and reinfection [20]. This study aims to investigate the impact of these factors on disease transmission dynamics and the effectiveness of control measures.

Mathematical models are indispensable for understanding the dynamics of infectious disease transmission and forecasting epidemic trajectories. In particular, models that account for

breakthrough infections and reinfection have been the subject of extensive study. In infectious disease modeling, breakthrough infections have been increasingly recognized as a critical factor shaping transmission dynamics and control effectiveness. Perkins et al. developed a stochastic dengue model, demonstrating the substantial impact of breakthrough infections on vaccination effectiveness and underscoring the need to integrate this factor into such models [21]. Azimaqin et al. proposed an age-structured model to investigate the 2015 mumps resurgence in China, linking the outbreak to vaccine failure, seasonal effects, and shifts in population structure [22]. Xu et al. established a dynamic transmission model using Chinese hepatitis B data, highlighting that increasing vaccination rates could significantly enhance disease control [23]. Elbasha et al. introduced a vaccination model with waning immunity, showing that backward bifurcation may occur when vaccine protection is partial and its duration falls below a critical threshold [24]. Yuliana et al. analyzed an SIVS model under vaccine failure, concluding that breakthrough infections substantially contribute to sustained high transmission [25]. Finally, Jing et al. developed a COVID-19 model incorporating breakthrough infection and age structure, emphasizing that high vaccine coverage combined with effective antiviral drugs is essential to achieve disease eradication [26].

In the study of reinfection in infectious disease modeling, several works have provided critical insights. Montalban et al. developed a herd immunity model incorporating individual heterogeneity and reinfection, demonstrating that epidemic growth can be effectively suppressed once the proportion of immune population exceeds the herd immunity threshold [27]. Rehman et al. proposed a fractional-order malaria model accounting for memory effects, relapse, and reinfection, identifying vaccination as a key factor in preventing disease recurrence [28]. Anggriani et al. introduced a multi-strain dengue model, showing that reinfection with the same serotype elevates both primary and secondary case numbers [29]. Gomes et al. compared SIR and SIS frameworks to evaluate the impact of post-recovery immunity, revealing that below the reinfection threshold, primary infections dominate with low incidence, whereas above it, reinfection drives high infection levels [30]. Agusto developed an Ebola model incorporating recurrence and reinfection, identifying reinfection as a trigger for backward bifurcation [31]. Rodrigues et al. assessed tuberculosis risks under partial immunity, indicating that the average reinfection rate may exceed that of primary infections [32]. In response to recurrent hepatitis B outbreaks, Megala et al. integrated reinfection with Crowley-Martin incidence and ongoing vaccination, underscoring the combined influence of vaccination, reinfection, and preventive measures on HBV transmission dynamics [33].

Extensive research has confirmed the critical role of breakthrough infections and rein-

fection in shaping disease dynamics and complicating control initiatives. Notably, several major infectious diseases—such as COVID-19, influenza, and dengue exhibit both phenomena concurrently. Nevertheless, existing modeling frameworks have largely failed to integrate these two mechanisms into a unified structure, leaving a notable gap in the development of effective and feasible intervention strategies. To address this limitation, we develop an epidemic model that simultaneously incorporates breakthrough infections and reinfection, and employ bang-bang optimal control as the central strategy for intervention design. A key advantage of the bang-bang approach lies in its "all-or-nothing" switching nature, which offers public health authorities clear, implementable, and resource efficient phased control policies. Our study aims not only to enhance the realism of disease transmission modeling but also to provide a theoretical foundation and practical strategy for deploying intensity-varying control measures in resource-constrained scenarios.

This paper is organized as follows. Firstly, an infectious disease model with breakthrough infection and reinfection is established, and we derive the basic reproduction number, prove the local stability of the disease-free equilibrium and the existence of backward bifurcations. Secondly, the theoretical results are verified by combining numerical simulations. Bang-Bang optimal control of the minimum-time problem is applied to the model to prove the existence of the optimal solution. Finally, a simulation research of Bang-Bang control is conducted to compare various control strategies to find the optimal strategy to control the disease in the shortest time.

2 Mathematical modelling

The population is divided into four categories, susceptible, vaccinated, infected, and recovered, with S(t), V (t), I(t), and R(t) representing the number of individuals in each class at time t. The disease transmission flow chart considering breakthrough infection and reinfection is shown in Fig1.

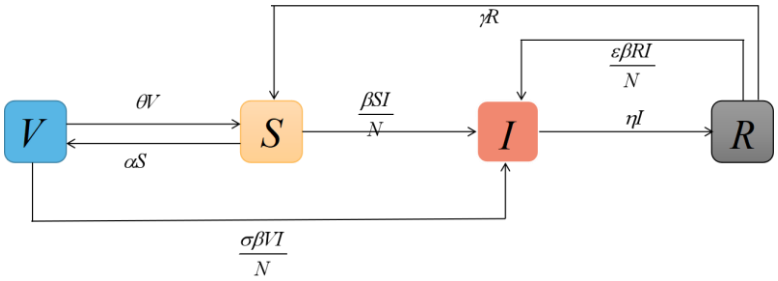

Fig. 1. Flow chart of disease transmission.

According to Fig1, the model can be expressed as

$$\begin{cases} \frac{dS}{dt} = -\frac{\beta SI}{N} - \alpha S + \theta V + \gamma R, \\ \frac{dV}{dt} = \frac{\sigma\beta VI}{N} - \theta V + \alpha S, \\ \frac{dI}{dt} = \frac{\beta(S+\sigma V+\epsilon R)I}{N} - \eta I, \\ \frac{dR}{dt} = \eta I - \frac{\beta\epsilon RI}{N} - \gamma R, \end{cases} \tag{1}$$

where $N = S + V + I + R$. The description of parameters in system (1) is given in Table1 .

System (1) incorporates breakthrough infection and reinfection into the dynamic system by introducing two key parameters. Breakthrough infection is characterized by the parameter $\sigma \in [0,\ 1]$, which represents the failure rate of the vaccine. When $\sigma = 0$, the vaccine provides complete protection, indicating no breakthrough infections; when $\sigma = 1$, vaccinated have the same risk of infection as susceptible. Reinfection is described by the parameter $\epsilon \in [0,\ 1]$, which represents the failure rate of natural immunity of recovered. $\epsilon > 0$ means that recovered may be reinfected due to incomplete or weakened immunity. Furthermore, the model also includes the process of waning immunity. Vaccinated lose vaccine-induced protection at a rate of θ, and recovered lose natural immunity at a rate of γ, both returning to the susceptible compartment. This system (1) characterizes both breakthrough infections and reinfections through the imperfectness and waning nature of immune protection.

Table 1. Description of parameters in system (1).

Parameters	Definition
β	The infection rate of infected
ϵ	The failure rate of the natural immunity of recovered
σ	The failure rate of vaccinated
α	The vaccination rate for susceptible
θ	The immunization loss rate of vaccinated
γ	The rate at which recovered become susceptible after natural immunity fails
η	Recovery rate of the infected

3 Basic reproduction number

Lemma 1 Assuming that the initial conditions $(S(0), V(0), I(0), R(0))$ of system (1) are non-negative, then

$$\Gamma = \left\{(S, V, I, R) \in R_4^+ \middle| 0 \le S + V + I + R = C\right\}^r,$$

is a positively invariant set for system (1), where C is a constant.

See Appendix for the proof process of Lemma 1.

Let $s = \frac{S}{N}$, $v = \frac{V}{N}$, $i = \frac{I}{N}$, $r = \frac{R}{N}$, then $s + v + i + r = 1$. Normalize system (1) and substituting $r = 1 - s - v - i$ into system (1), we obtain,

$$\begin{cases} \frac{ds}{dt} = -\beta si - \alpha s + \theta v + \gamma(1 - s - v - i), \\ \frac{dv}{dt} = -\sigma\beta vi - \theta v + \alpha s, \\ \frac{di}{dt} = \beta\left[s + \sigma v + \epsilon(1 - s - v - i)\right] i - \eta i. \end{cases} \tag{2}$$

Obviously, the positive invariant set of system (2) is $\Omega = \left\{(s, v, i) \in R_3^+ | 0 \le s + v + i \le 1\right\}$. This paper will analyze the system (2). It explains that system (2) is equivalent to system (1).

Let the right side of system (2) equal to 0, and we can get the disease-free equilibrium $P_0 = \left(\frac{\theta}{\alpha+\theta}, \frac{\alpha}{\alpha+\theta}, 0\right)$. Next, we use the next generation matrix method to give the basic reproduction number of system (2) [34]. First, consider the following two vectors

$$f = \begin{bmatrix} 0 \\ 0 \\ \beta\left[s + \sigma v + \epsilon(1 - s - v - i)\right] i \end{bmatrix}, g = \begin{bmatrix} \beta si + \alpha s - \theta v - \gamma(1 - s - v - i) \\ \sigma\beta vi + \theta v - \alpha s \\ \eta i \end{bmatrix},$$

The Jacobian matrices of vectors f and g at the disease-free equilibrium P_0 are

$$F = \begin{bmatrix} 0 & 0 & 0 \\ 0 & 0 & 0 \\ 0 & 0 & \frac{\beta(\sigma\alpha+\theta)}{\alpha+\theta} \end{bmatrix}, G = \begin{bmatrix} \alpha+\gamma & -\theta+\gamma & \frac{\beta\theta}{\alpha+\theta}+\gamma \\ -\alpha & \theta & \frac{\beta\sigma\alpha}{\alpha+\theta} \\ 0 & 0 & \eta \end{bmatrix}.$$

The inverse of the matrix G is

$$G^{-1} = \begin{bmatrix} \frac{\theta}{\gamma(\alpha+\theta)} & \frac{\theta-\gamma}{\gamma(\alpha+\theta)} & \frac{-(\beta+\gamma)\theta^2-(\beta\sigma+\gamma)\alpha\theta+\alpha\beta\gamma\sigma}{\gamma(\alpha+\theta)^2\eta} \\ \frac{\alpha}{\gamma(\alpha+\theta)} & \frac{\alpha+\gamma}{\gamma(\alpha+\theta)} & -\frac{\alpha[(\beta\sigma+\gamma)\alpha+(\beta\sigma+\theta)\gamma+\beta\theta]}{\gamma(\alpha+\theta)^2\eta} \\ 0 & 0 & \frac{1}{\eta} \end{bmatrix},$$

Then, accoroding to the next generation approach, the basic reproduction number is given as $R_0 = \rho(FG^{-1}) = \frac{\beta(\sigma\alpha+\theta)}{\eta(\alpha+\theta)}$.

4 Stability of disease-free equilibrium

Theorem 1 When $R_0 < 1$, the disease-free equilibrium P_0 of system (2) is locally asymptotically stable. When $R_0 = 1$ and $R_0 \neq R_*$ $\left(R_* = \frac{[(\alpha\sigma+\theta)(\gamma+\eta)+\gamma\eta\sigma](\alpha\sigma+\theta)}{\eta(\alpha+\theta)[(\alpha\sigma+\theta)\epsilon+\gamma\sigma]}\right)$, the disease-free equilibrium P_0 is a saddle node. When $R_0 = 1$ and $R_0 = R_*$, the disease-free equilibrium P_0 is a stable node. When $R_0 > 1$, the disease-free equilibrium P_0 of system (2) is unstable.

See Appendix for the proof process of Theorem1.

5 Existence of endemic equilibria

First, let the right side of system (2) equal to 0,

$$\begin{cases} -\beta si - \alpha s + \theta v + \gamma(1 - s - v - i) = 0, \\ -\sigma\beta vi - \theta v + \alpha s = 0, \\ \beta\left[s + \sigma v + \epsilon(1 - s - v - i)\right] i - \eta i = 0. \end{cases} \tag{3}$$

Solving equations (3) yields

$$s = \frac{(\beta i\sigma + \theta)\gamma(1 - i)}{\beta^2 i^2\sigma + \beta(\alpha\sigma + \gamma\sigma + \theta)i + \gamma(\alpha + \theta)}, v = \frac{\alpha\gamma(1 - i)}{\beta^2 i^2\sigma + \beta(\alpha\sigma + \gamma\sigma + \theta)i + \gamma(\alpha + \theta)}. \tag{4}$$

Substituting formula (4) into the third equation of system (3) yields

$$F(i) = b_3 i^3 + b_2 i^2 + b_1 i + b_0 = 0, \tag{5}$$

where

$$b_3 = \beta^3\epsilon\sigma > 0, b_2 = \beta^2\left[(-\beta\epsilon + \alpha\epsilon + \eta + \gamma)\sigma + \epsilon\theta\right],$$

$$b_1 = \beta\left[\sigma(\gamma(\eta - \beta + \alpha) + \alpha(-\epsilon\beta + \eta)) + \theta(-\epsilon\beta + \eta + \gamma)\right], b_0 = \gamma\eta(\alpha + \theta)(1 - R_0).$$

5.1 Case $R_0 = 1$

Next, We first discuss case $R_0 = 1$ in which

$$b_0 = 0, b_1 = \frac{(\alpha + \theta)\eta}{(\sigma\alpha + \theta)^2}\left[(\eta + \gamma)(\alpha\sigma + \theta)^2 + \alpha\gamma(\sigma^2 - \sigma) - \eta(\alpha + \theta)(\alpha\sigma + \theta)\epsilon\right],$$

$$b_2 = \frac{(\alpha + \theta)^2\eta^2}{(\sigma\alpha + \theta)^3}\left[(\alpha\sigma + \theta)(\eta + \gamma)\sigma + (\alpha\sigma + \theta)^2\epsilon - \epsilon\eta\sigma(\alpha + \theta)\right],$$

the roots of equation (5) are

$$i_{01} = \frac{-b_2 + \sqrt{b_2^2 - 4b_1 b_3}}{2b_3}, i_{02} = \frac{-b_2 - \sqrt{b_2^2 - 4b_1 b_3}}{2b_3}, i_{03} = 0.$$

(a) If $b_1 < 0$, then $R_0 > R_*$ and $i_{02} < 0$. Equation (5) has a unique positive root i_{01}. It is obvious that $i_{01} \in [0, 1]$. Then system (2) has an endemic equilibrium P_3 in Ω, where

$$P_3 = \left(\frac{(\beta i_{01}\sigma + \theta)\gamma(1 - i_{01})}{\beta^2 i_{01}^2\sigma + \beta(\alpha\sigma + \gamma\sigma + \theta)i_{01} + \gamma(\alpha + \theta)}, \frac{\alpha\gamma(1 - i_{01})}{\beta^2 i_{01}^2\sigma + \beta(\alpha\sigma + \gamma\sigma + \theta)i_{01} + \gamma(\alpha + \theta)}, i_{01}\right).$$

(b) If $b_1 = 0$, then $R_0 = R_*$, that is $(\alpha\sigma + \theta)(\gamma + \eta) = \frac{\eta(\alpha+\theta)(\alpha\sigma+\theta)\epsilon + \alpha\gamma(\sigma-\sigma^2)}{\alpha\sigma+\theta}$, $b_2 = \frac{(\alpha+\theta)^2\eta^2}{(\alpha\sigma+\theta)^3}\left(\alpha\gamma\sigma(\sigma - \sigma^2) + (\alpha\sigma + \theta)^2\epsilon\right)$. Therefore, $b_2 \geq 0$. Furthermore, it can be seen that equation (5) does not have any positive roots.

(c) If $b_1 > 0$, then $R_0 < R_*$, $(\alpha\sigma + \theta)(\gamma + \eta) > \frac{\eta(\alpha+\theta)(\alpha\sigma+\theta)\epsilon + \alpha\gamma(\sigma-\sigma^2)}{\alpha\sigma+\theta}$. So

$$b_2 > \frac{(\alpha + \theta)^2\eta^2}{(\alpha\sigma + \theta)^3}\left[\frac{\alpha\gamma\sigma(\sigma - \sigma^2)}{\alpha\sigma + \theta} + (\alpha\sigma + \theta)^2\epsilon\right] \geq 0.$$

Therefore, equation (5) does not have any positive roots.

5.2 Case $R_0 < 1$

When $R_0 < 1$, $b_0 > 0$. The necessary and sufficient conditions for $b_1 = 0$ is $R_0 = R_*$.

(a)If $R_* > 1$, then $0 < R_0 < 1 < R_*$, $b_1 > 0$. Furthermore $\beta < \frac{(\alpha\sigma+\theta)(\gamma+\eta)+\gamma\eta\sigma}{(\alpha\sigma+\theta)\epsilon+\gamma\sigma}$,

$$> \left(\frac{1}{(\alpha\sigma+\theta)\epsilon+\gamma\sigma}\right)\{(\alpha\sigma+\theta)^2\epsilon^2+\gamma\sigma(\alpha\sigma+\theta)\epsilon+\gamma^2\sigma^2+\eta\gamma\sigma^2(1-\epsilon)\}^r \geq 0.$$

Therefore, $b_2 \geq 0$. It can be seen that equation (5) does not have any positive roots.

(b) If $R_0 < R_* = 1$, then $b_1 = 0$, further $b_2 \geq 0$, so equation (5) does not have positive roots.

(c) If $R_* < 1$.

When $0 < R_0 < R_* < 1$, $b_1 > 0$, it has $b_2 \geq 0$. So equation (5) does not have positive roots.

When $0 < R_* < R_0 < 1$, $b_1 < 0$, taking partial derivatives of both sides of equation (5) with respect to i, we can obtain

$$G(i) = 3b_3i^2 + 2b_2i + b_1 = 0. \tag{6}$$

The two real roots of equation (6) are

$$i_{11} = \frac{-b_2 + \sqrt{b_2^2 - 3b_1b_3}}{3b_3}, \; i_{12} = \frac{-b_2 - \sqrt{b_2^2 - 3b_1b_3}}{3b_3}.$$

Then the necessary and sufficient conditions for the existence of positive roots of equation (5) is $b_3i_{11}^3 + b_2i_{11}^2 + b_1i_{11} + b_0 \leq 0$, that is, $R_0 \geq R_{**}$, where

$$R_{**} = 1 + \frac{\left(-b_2 + \sqrt{-3b_1b_3 + b_2^2}\right)\left(6b_1b_3 - b_2^2 + b_2\sqrt{-3b_1b_3 + b_2^2}\right)}{27b_3^2\gamma\eta(\alpha+\theta)} \; (R_{**} < 1).$$

If $R_0 < R_{**}$, $b_3i_{11}^3 + b_2i_{11}^2 + b_1i_{11} + b_0 > 0$. Thus, equation (5) does not have positive roots.

When $0 < R_* < R_0 < 1$ and $R_0 = R_{**}$, it has $b_1 < 0$ and $b_3i_{11}^3 + b_2i_{11}^2 + b_1i_{11} + b_0 = 0$. Therefore, equation (5) has a positive root i_1, as shown in Fig2(a), and system (2) has an endemic equilibrium P_1 in Ω, where

$$P_1 = \left(\frac{(\beta i_{11}\sigma+\theta)\gamma(1-i_{11})}{\beta^2i_{11}^2\sigma+\beta(\alpha\sigma+\gamma\sigma+\theta)i_{11}+\gamma(\alpha+\theta)}, \frac{\alpha\gamma(1-i_{11})}{\beta^2i_{11}^2\sigma+\beta(\alpha\sigma+\gamma\sigma+\theta)i_{11}+\gamma(\alpha+\theta)}, i_{11}\right),$$

$$i_{11} = \frac{-b_2+\sqrt{b_2^2-3b_1b_3}}{3b_3}, \; i_{11} \in [0,1]$$

When $0 < R_* < R_0 < 1$ and $R_0 > R_{**}$, it has $b_1 < 0$ and $b_3i_1^3 + b_2i_1^2 + b_1i_1 + b_0 < 0$. Then, equation (5) has three different real roots, as shown in Fig2(b). One of them is negative, and the other two are positive real roots, namely i_2 and i_3.

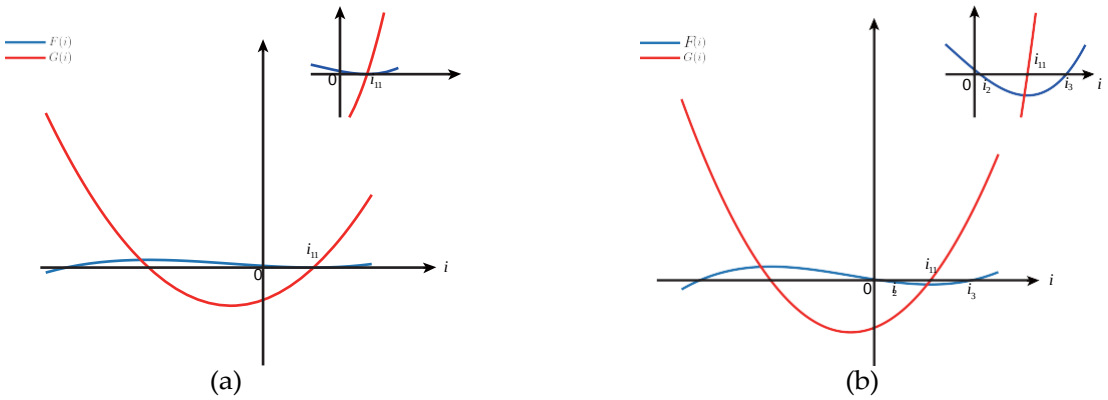

Fig. 2. When $R_* < R_0 < 1$, the existence of the root of equation (5) under different conditions. (a) $R_0 = R_{**}$, (b) $R_0 > R_{**}$.

Therefore, system (2) has two endemic equilibrium P_2 and P_3 respectively

$$P_2 = \left(\frac{(\beta i_2\sigma + \theta)\gamma(1 - i_2)}{\beta^2 i_2^2\sigma + \beta(\alpha\sigma + \gamma\sigma + \theta)i_2 + \gamma(\alpha + \theta)}, \frac{\alpha\gamma(1 - i_2)}{\beta^2 i_2^2\sigma + \beta(\alpha\sigma + \gamma\sigma + \theta)i_2 + \gamma(\alpha + \theta)}, i_2 \right),$$

$$P_3 = \left(\frac{(\beta i_3\sigma + \theta)\gamma(1 - i_3)}{\beta^2 i_3^2\sigma + \beta(\alpha\sigma + \gamma\sigma + \theta)i_3 + \gamma(\alpha + \theta)}, \frac{\alpha\gamma(1 - i_3)}{\beta^2 i_3^2\sigma + \beta(\alpha\sigma + \gamma\sigma + \theta)i_3 + \gamma(\alpha + \theta)}, i_3 \right).$$

When $i = 1$, $F(1) = \eta\,[\beta^2\sigma + (\alpha\sigma + \gamma\sigma + \theta)\beta + \gamma(\alpha + \theta)] > 0$, so $i_2, i_3 \in [0, 1]$.

5.3 Case $R_0 > 1$

In this section, we will discuss the existence of endemic equilibria in system (2) when $R_0 > 1$. If $R_0 > 1$, then $b_0 < 0$. It is clear that equation (5) has at least one positive root.

(i) If $R_* \geq R_0 > 1$, then $b_1 > 0$, $b_2 > 0$. As shown in Fig3(b)-(c), in the positive semi-axis region of the x-axis, F(i) will monotonically increase from b_0 and cross the x-axis into the first quadrant, so equation (5) has a positive root.

(ii) If $R_* < R_0$, then $b_1 < 0$. As shown in Fig3(a), in the positive half-axis region of the x-axis, F(i) is a concave function. It initially decreases monotonically from $b_0(b_0 < 0)$ to a limit, and then increases to a positive value. It is easy to see that equation (5) has only one positive root i_1^*.

When $i = 1$, since $F(1) > 0$. In summary, when $R_0 > 1$, system (2) has a endemic equilibrium P_3 in Ω.

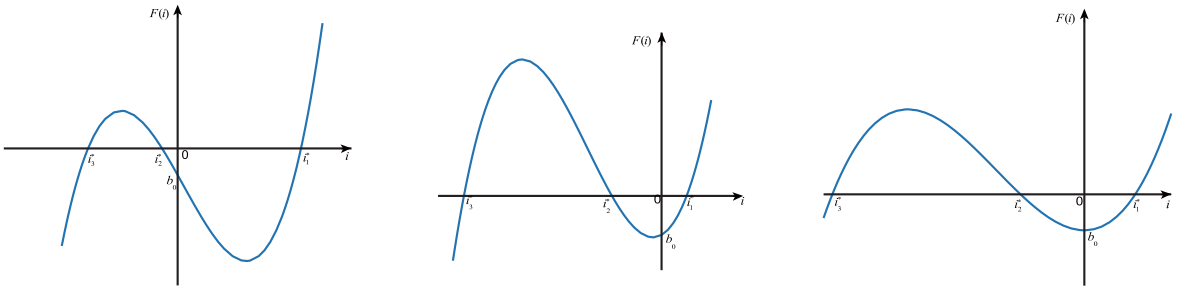

(a) (b) (c)

Fig. 3. When $R_0 > 1$, the existence of the root of equation (5) under different conditions. (a) $R_* < R_0$, (b) $R_* > R_0$, (c) $R_* = R_0$.

6 Stability of endemic equilibria

Theorem 2 When $R_{**} < R_0 < 1$ and $R_* < R_0$, the endemic equilibrium P_2 of system (2) is unstable.

See Appendix for the proof process of Theorem2.

Theorem 3 If $\sigma = 0$, when $R_* \geq 1$ and $R_0 > 1$, or $R_{**} < R_0$, $R_* < R_0$ and $R_* < 1$, the endemic equilibrium P_3 of system (2) is locally asymptotically stable.

See Appendix for the proof process of Theorem3.

Next, the existence and stability conditions of equilibria of system(2)under different conditions are summarized in Table 2.

Table 2. Existence and stability of equilibria of system(2).

Conditions		Existence of equilibria	Stability of equilibria
$R_* \geq 1$	$0 < R_0 \leq 1$	Disease-free equilibrium P_0	P_0 is stable
	$R_0 > 1$	Disease-free equilibrium P_0, The only endemic equilibrium P_3	P_3 is stable
$R_* < 1$	$R_{**} = R_0 < 1, R_* < R_0$	Disease-free equilibrium P_0, The only endemic equilibrium P_1	\
	$R_{**} < R_0 < 1, R_* < R_0$	Disease-free equilibrium P_0, Two endemic equilibria P_2, P_3	P_0 and P_3 are bistable
	$R_0 = 1$	Disease-free equilibrium P_0, Endemic equilibrium P_3	P_3 is stable
	$R_0 > 1$	Disease-free equilibrium P_0, Endemic equilibrium P_3	P_3 is stable
	$0 < R_0 < R_{**}$	Disease-free equilibrium P_0	P_0 is stable

7 Numerical simulation

In this section, we will verify the theoretical results in Section 6 through numerical simulations. From Fig 4, we can see that when $R_0 = 1$ and $R_* \geq 1$, the disease-free equilibrium P_0 is stable. When $R_0 = 1$ and $R_* < 1$, the disease-free equilibrium P_0 is unstable, and the endemic equilibrium P_3 is stable. From Fig 5, we can see that when $R_0 < 1$, $R_* \geq 1$ or $R_* < 1$ and $R_{**} > R_0$, the disease-free equilibrium P_0 is stable. When $R_* < 1$ and $R_{**} = R_0 < 1$, the disease-free equilibrium P_0 and the endemic equilibrium P_1 are bistable. When $R_* < 1$ and $R_{**} < R_0 < 1$, the endemic equilibrium P_2 is unstable, P_0 and P_3 are bistable.

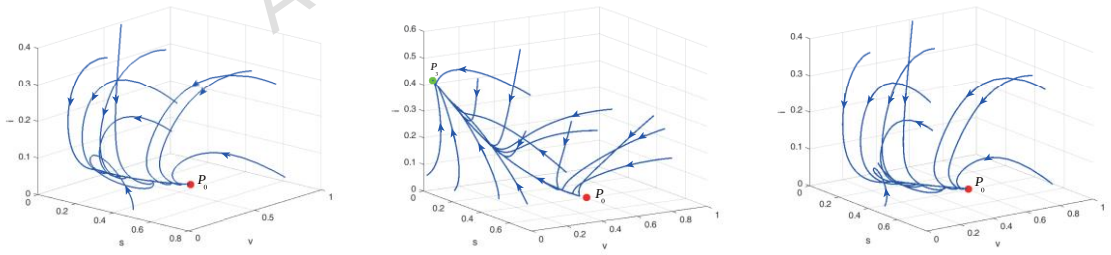

(a) (b) (c)

Fig. 4. When $R_0 = 1$, the phase diagram of system (2) under different conditions. (a) $R_* = 1$. (b) $R_* < 1$. (c) $R_* > 1$. The red dots represent the disease-free equilibrium P_0, and the green dots represent the endemic equilibrium P_3. The values of the parameters are given in the text, as well as in other figures.

Next, we use the Matcont package in Matlab to draw the bifurcations diagram of system (2). We set the parameters as $\beta = 0.25$, $\epsilon = 0.8$, $\sigma = 0.1$, $\theta = 0.001$, $\gamma = 0.05$, $\eta = \frac{1}{7}$, $\alpha = 0.01$.

Then, $R_0 = 0.9625 < 1$, $R_* = 0.7911 < 1$. The corresponding backward bifurcations diagram is shown in Fig 6(b). Taking parameters $\epsilon = 0.3$, $R_0 = 0.9625 < 1$, $R_* = 1.3154 > 1$, the corresponding forward bifurcations diagram is shown in Fig 6(a). From Fig 7, we can see that when σ and ϵ are very small, that is, when the breakthrough infection and reinfection rates are very low, the disease will be extinct and will not become endemic. When the initial value is set to $(0.5, 0.4, 0.08)$, Fig 8 shows the change of infected people over time under different values of σ and ϵ. When the parameter value exceeds the red interface or the value of the red dotted line, the disease will break out on a large scale, otherwise the disease will be a small epidemic or extinction. When the disease is prevalent, improving the immunity of the vaccine and reducing breakthrough infection play a vital role in epidemic prevention and control. Strengthening the natural immunity of the recovered and reducing the reinfection rate can reduce the final epidemic scale of the disease, but the disease cannot be eradicated.

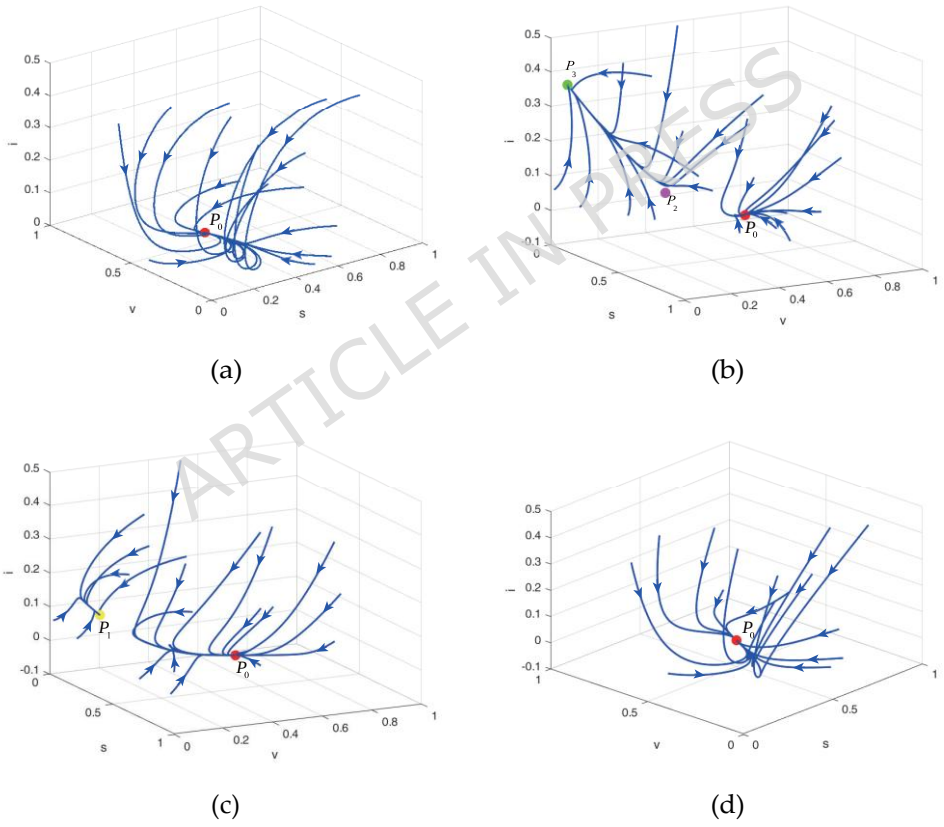

Fig. 5. When $R_0 < 1$, the phase diagram of system (2) under different conditions. (a) $R_* \geq 1$. (b) $R_* < 1$ and $R_{**} < R_0$. (c) $R_* < 1$ and $R_{**} = R_0$. (d) $R_* > 1$ and $R_{**} = R_0$. The red point represents the disease-free equilibrium P_0, and the yellow, purple and green points represent the endemic equilibria P_1, P_2 and P_3, respectively.

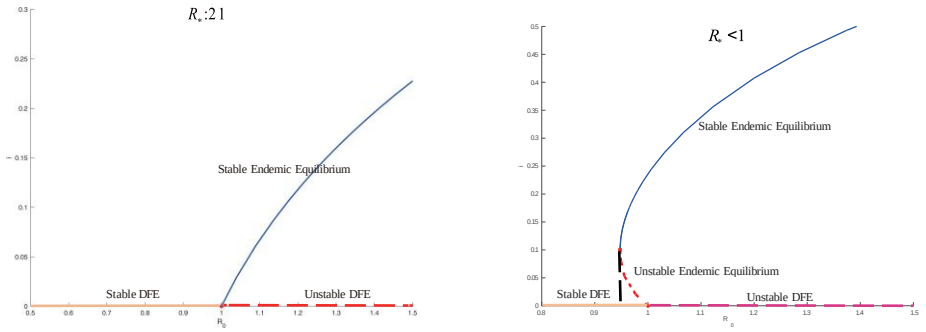

(a) (b)

Fig. 6. Bifurcations diagrams under different conditions. (a) $R_* \geq 1$. (b) $R_* < 1$. The dotted line indicates an unstable equilibrium , and the solid line indicates a stable equilibrium.

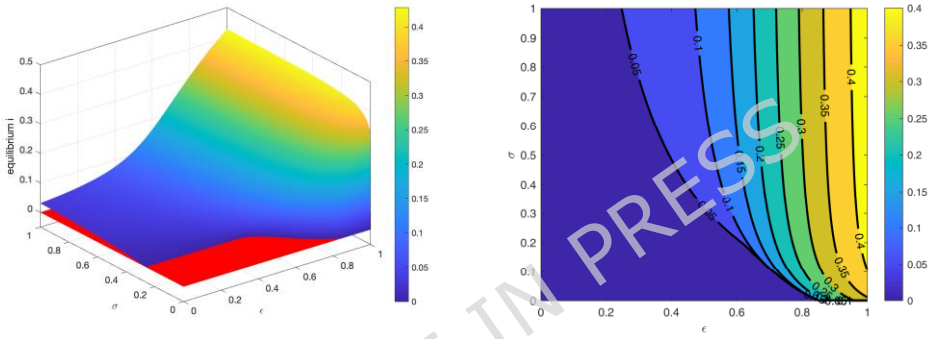

(a) (b)

Fig. 7. The change of equilibrium i under different σ and ϵ. The equilibrium in the red area is equal to 0.

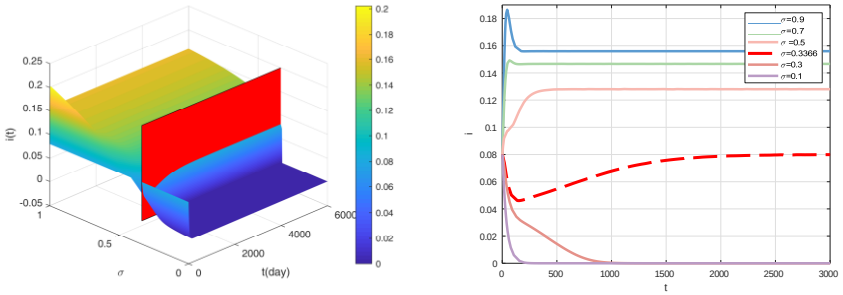

(a) (b)

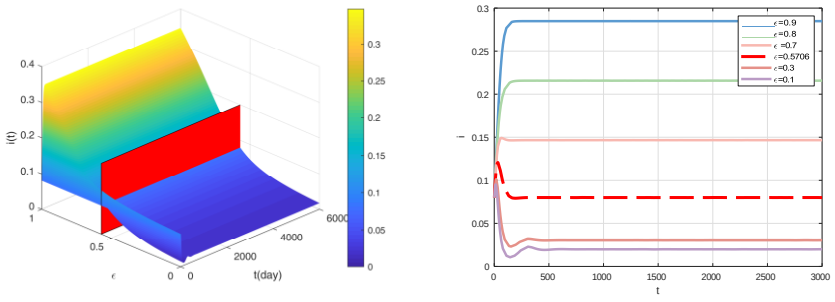

(c) (d)

Fig. 8. The change of infected i(t) over time under different σ and ϵ.

When $\sigma = 0$, $R_* = \frac{\theta(\gamma+\eta)}{\eta(\alpha+\theta)\epsilon}$. When $\epsilon = 0$, $R_* = \frac{[(\alpha\sigma+\theta)(\gamma+\eta)+\gamma\eta\sigma](\alpha\sigma+\theta)}{\gamma\eta\sigma(\alpha+\theta)}$. Take $\theta = 0.005$, then $R_0 = 2.56$. From Fig9, we can see that when at least one of σ and ϵ is not 0, system (2) may have a backward bifurcations. However, when σ and ϵ are both 0, system (2) will have no backward bifurcations.

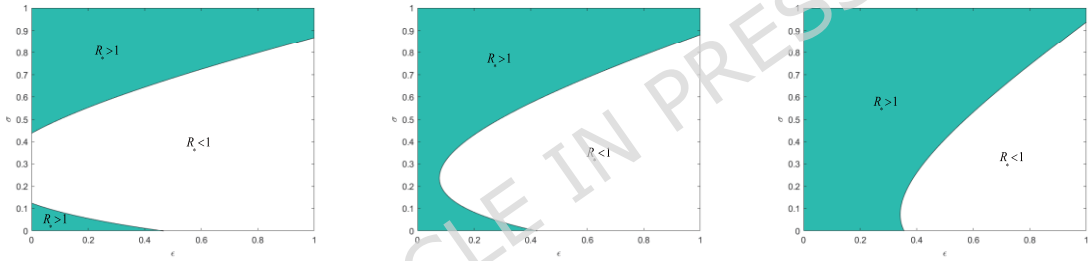

(a) (b) (c)

Fig. 9. Relationship between σ, ϵ and R_* under different conditions. (a) $\gamma = 0.05$. (b) $\gamma = 0.0333$. (c) $\gamma = 0.0083$.

8 Optimal control

In this section, we will investigate a formalized time control problem. First, we propose a definition of disease eradication time for an infectious disease system.

Definition 1 The disease eradication time T of an infectious disease system is the moment when the number of infected first reaches a threshold k ($0 < k < \frac{1}{N}$), where N is the total population.

In order to make Definition 1 meaningful, we choose the initial value of the number of infected in system (2) to be strictly greater than k. T is the time when the number of infected i(t) drops to k for the first time, that is, $T = \inf\{t > 0 | i(t) = k\}$. From a biological perspective,

setting the condition $k < \frac{1}{N}$ to determine the disease eradication time means that the disease will become extinct when the number of infected is less than 1.

Based on system (7), the following three parameters are considered as control variables

(i) $u_1(t) \in U$ indicates the percentage of infection rate reduction due to reduced detection by wearing masks, maintaining social distance, et al.

(ii) $u_2(t) \in U$ indicates increasing vaccination rates among susceptible;

(iii) $u_3(t) \in U$ indicates that the protection rate of the vaccine is improved.

Where $U = \{u_1, u_2, u_3 | 0 \le u_1, u_2, u_3 \le 1\}$ is control set. Our goal is to eradicate the disease in the shortest possible time. The corresponding state equation is

$$\begin{cases} \frac{ds}{dt} = -(1-u_1)\beta si - u_2 s + \theta v + \gamma(1-s-v-i), \\ \frac{dv}{dt} = -(1-u_1)(1-u_3)\sigma\beta vi - \theta v + u_2 s, \\ \frac{di}{dt} = (1-u_1)\beta[s + (1-u_3)\sigma v + \epsilon(1-s-v-i)]i - \eta i. \end{cases} \tag{7}$$

Let $\vec{x}(t) = (s(t), v(t), i(t))$, $\vec{u}(t) = (u_1(t), u_2(t), u_3(t))^T$,

$$\vec{f}(t, \vec{x}, \vec{u}) = \begin{bmatrix} -(1-u_1)\beta si - u_2 s + \theta v + \gamma(1-s-v-i) \\ -(1-u_1)(1-u_3)\sigma\beta vi - \theta v + u_2 s \\ (1-u_1)\beta[s + (1-u_3)\sigma v + \epsilon(1-s-v-i)]i - \eta i \end{bmatrix},$$

then, system (7) can be rewritten as $\vec{x}' = \vec{f}(t, \vec{x}, \vec{u})$, $\vec{x}(0) = x^0$. For system (7), we set the initial conditions to $i(0) > k$, $s(0) > 0$ or $v(0) > 0$. Under this initial condition, the solution of system (7) is represented by $\vec{x}(t)$, and its set is marked as X.

Eradicating the disease in the shortest possible time is of great significance. To achieve this goal, we study the following time optimal control problem: $J(u) = \mathbf{min} \int_0^T 1dt, i(T) = k$.

8.1 Existence of the optimal solution

Next, according to Theorem 4.1 and the corollary method in reference [35], we prove that system (7) has sufficient conditions for optimal control. This is shown in Lemma 2 below.

Lemma 2 For the time optimal control problem, there exists an optimal control $\vec{u}^*(t)$.

See Appendix for the proof process of Lemma 2.

Theorem 4 If $\vec{u}^*(t)$ is the minimum value of the time-optimal control problem, then $\vec{u}^*(t)$ isa Bang-Bang control.

See Appendix for the proof process of Theorem3.

8.2 Simulation of optimal control

In this summary, we use the fmincon function to simulate Bang-Bang control. Here, the initial value and parameter values of system (2) in the simulation research are set as $s(0) = 0.4$,

$v(0) = 0.5$, $i(0) = 0.1$, $\beta = 0.9$, $\epsilon = 0.4$, $\sigma = 0.1$, $\theta = 0.02$, $\gamma = 0.001$, $\eta = 0.1667$, $\alpha = 0.01$ $k = 1 \times 10^{-3}$. Then, $R_0 = 3.7792 > 1$. In real life, every control measure cannot reach 100%, so it is assumed that $u_{imin} = 0$, $u_{imax} = 0.98$, where $i = 1, 2, 3$. The control goal is to control the spread of the disease as much as possible in the shortest time. Next, the disease prevalence under various control measures is compared to find the best prevention and control measure. Fig11-Fig17 show the dynamic changes of infected under no control measures and different control measures. Table3 shows the disease control time and cumulative infection proportion corresponding to each control measure.

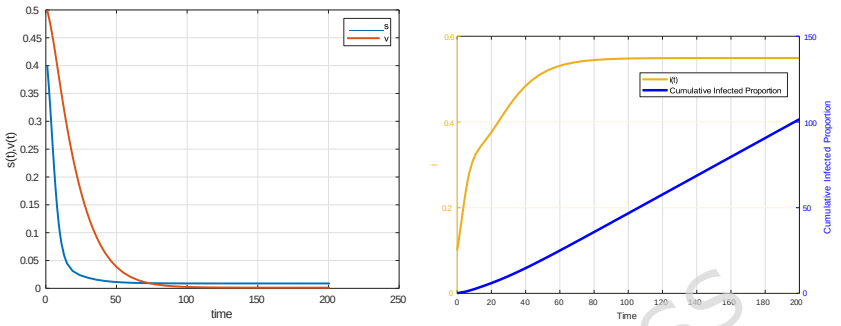

(a) (b)

Fig. 10. Without any control measures, the changes of state variables s, v, and i over time.

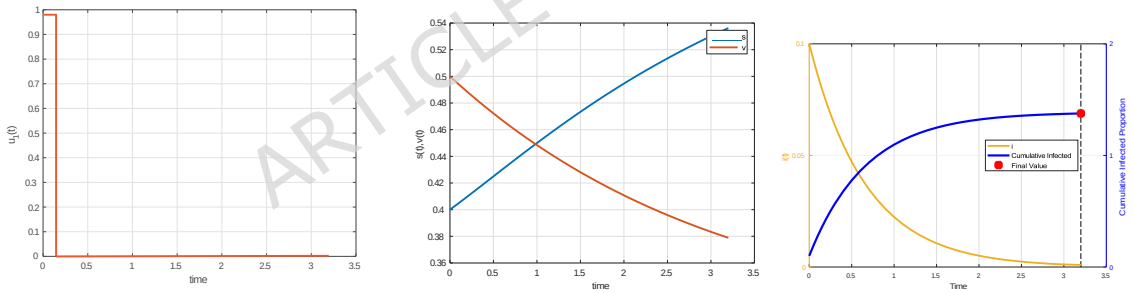

(a) (b) (c)

Fig. 11. Considering only the control of the infection rate, the changes of the control variable u_1 and the state variables s, v, i over time.

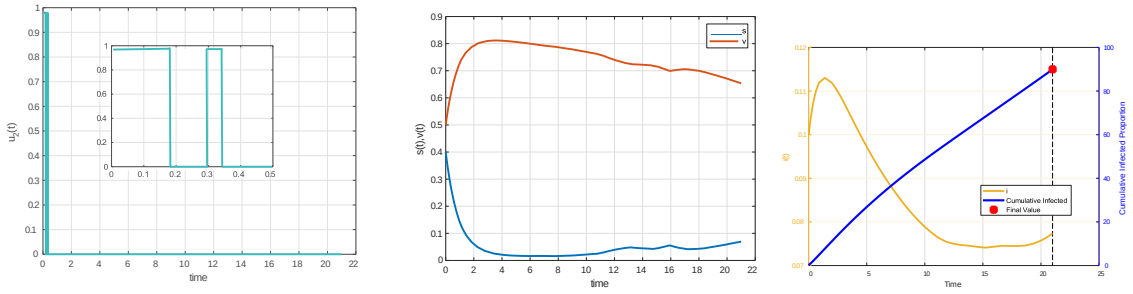

(a) (b) (c)

Fig. 12. Considering only the vaccination rate, the change of control variable u_2 and state variables s, v, i over time.

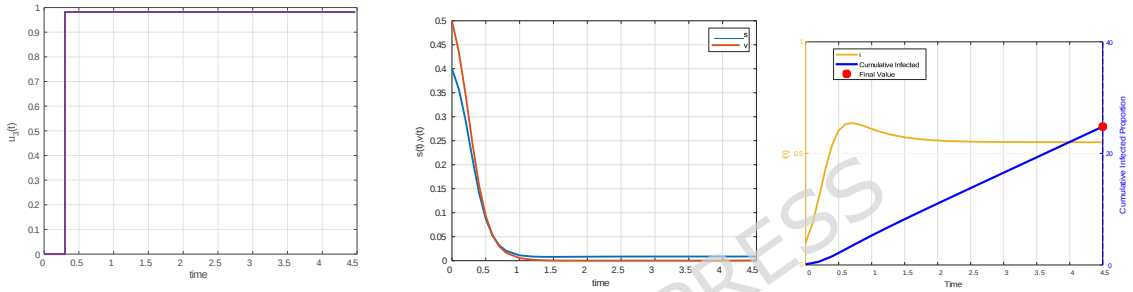

(a) (b) (c)

Fig. 13. Considering only the control of vaccine protection rate, the change of control variable u_3 and state variables s, v, i over time.

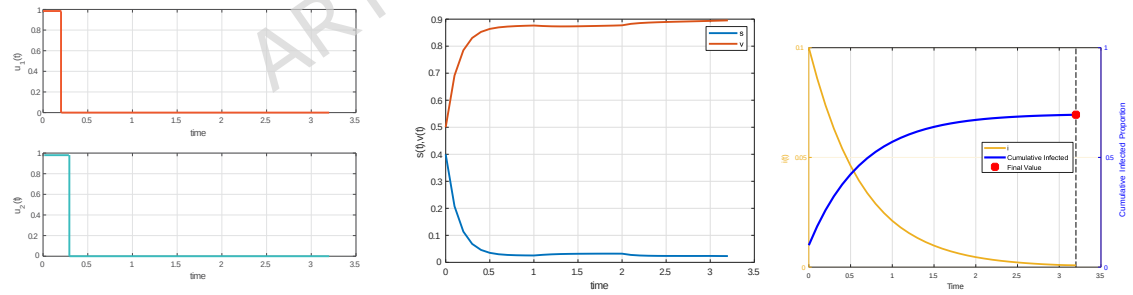

(a) (b) (c)

Fig. 14. Considering the control of infection rate and vaccination rate, the change of control variables u_1, u_2 and state variables s, v, i over time.

From Fig10, we can see that if no control measures are taken, the disease will become endemic with a high prevalence trend. When only the vaccination rate is increased without implementing other control strategies, as shown in Fig12, the disease will be controlled in a short period of time, but the vaccine protection rate will gradually weaken over time, and the

negligence of protective measures will cause the recurrence of the disease. However, even if the vaccine protection rate is increased for a long time without strengthening the vaccination rate through publicity and education, as shown in Fig13, the disease will not be controlled, it will continue to exist and become endemic. As shown in Fig11, if social distance, mask wearing, and reduced outdoor activities are taken in the short term, the epidemic can be effectively controlled at time t = 3.15. From Fig14-Fig16, we can see that the disease can be quickly controlled when two control strategies are considered simultaneously. Among them, controlling the infection rate and increasing the vaccination rate take the shortest time to reach the control target, while controlling the infection rate and increasing the vaccine protection rate take the longest time to reach the control target, and it takes a period of time in the early stage to be controlled, which may be related to the relatively low vaccination rate.

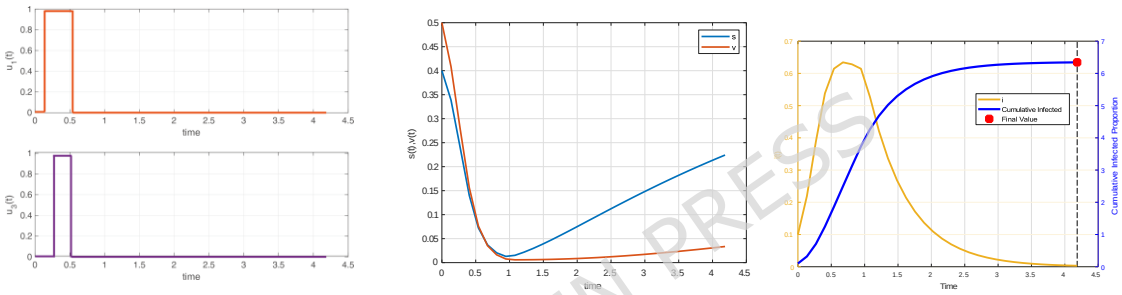

(a) (b) (c)

Fig. 15. Considering the control of infection rate and vaccine protection rate, the change of control variables u_1, u_3 and state variables s, v, i over time.

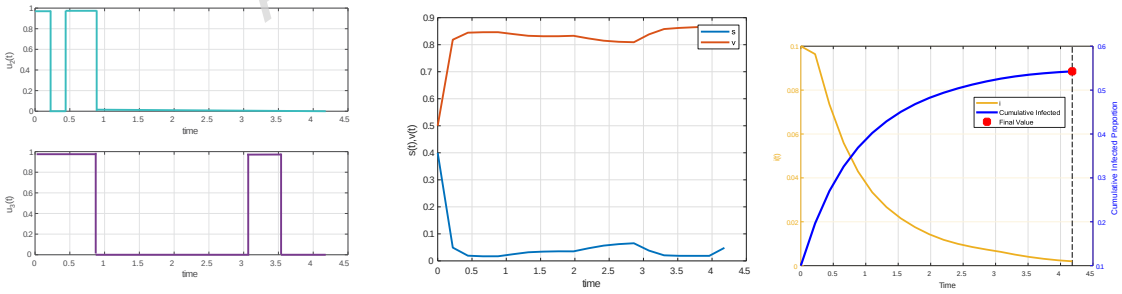

(a) (b) (c)

Fig. 16. Considering the control of vaccination rate and protection rate, the change of control variables u_2, u_3 and state variables s, v, i over time.

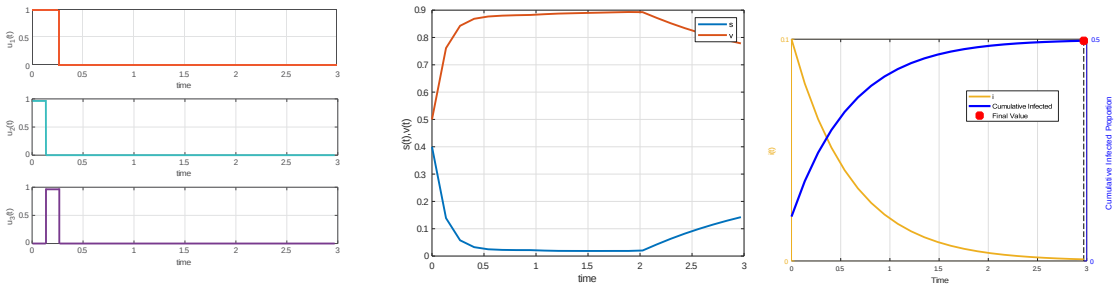

(a) (b) (c)

Fig. 17. Considering all control measures, the changes of control variables u_1, u_2, u_3 and state variables s, v, i over time.

Table 3. Duration of disease control and cumulative infection Proportion in different control measures.

Case	Control Strategy	Control Time	Cumulative Infected Proportion
1	u_1	3.15	1.38
2	u_2	-	-
3	u_3	-	-
4	u_1, u_2	3.0	0.69
5	u_1, u_3	4.19	6.34
6	u_2, u_3	4.18	0.54
7	u_1, u_2, u_3	2.83	0.49

If the three control measures are considered at the same time, as shown in Fig17, it can be found that the control target is achieved at time t = 2.835, and the control time is often shorter. Table3 shows that by implementing all control strategies, the disease containment target can be achieved in the shortest possible time while minimizing the cumulative infection scale. Therefore, in order to control the spread of the disease in the short term, when the epidemic comes, it must strengthen the propaganda of infectious disease prevention and control, and reduce contact with infected people through non-drug intervention measures such as wearing masks, maintain social distance, and reduce going out, especially for patients in the recovery period to prevent secondary outbreaks. With the continuous emergence and threat of new and recurrent infectious diseases, in order to prevent and control the spread of diseases in the long term, it is necessary to develop infectious disease vaccines with high immunity, so as to effectively prevent and control the continuous occurrence of diseases. Although the long-term

implementation of prevention and control measures can curb the continuous spread of diseases, it will also cause waste of resources and even seriously interfere with the normal operation of the economy and society. However, Bang-Bang control provides an effective strategy, which can achieve the effect of disease prevention and control by implementing prevention and control strategies in a very short time.

9 Conclusion

In order to investigate the impact of breakthrough infection and reinfection on the continuous outbreak of infectious diseases, a disease transmission model with breakthrough infection and reinfection is established. First, a dynamic analysis of the model is conducted. The basic reproduction number R_0 is obtained by using the next generation matrix method. The local stability of disease-free equilibrium when $R_0 < 1$ is proved. By analyzing the stability of disease-free equilibrium when $R_0 = 1$ and the existence of multiple endemic equilibria, we find that when $R_* < 1$, system (1) exhibits a backward bifurcation, which means that R_0 is no longer the threshold for judging whether the disease will persist or not. Secondly, the local stability of the endemic equilibrium P_2 and the instability of P_3 under certain conditions are proved. Numerical simulations show that backward bifurcation occurs in system (1) when at least one of the parameters σ (breakthrough infection) or ϵ (reinfection) is non-zero. Obviously, breakthrough infection and reinfection play a vital role in the multiple outbreaks of the disease. When σ and ϵ approach 0, the disease will be effectively controlled and will not evolve into an endemic disease. On the contrary, the disease will spread extensively and eventually become an endemic disease when at least one of σ or ϵ approaches to 1. In the context of pandemic control, real-world conditions such as resource constraints and socioeconomic factors often limit the long-term continuous implementation of intervention measures. Therefore, this study attempts to explore feasible pathways for dynamically switching different prevention and control methods within a limited period, based on the Bang-Bang control strategy under a discrete control framework. Finally, Bang-Bang control is used to conduct an optimization control, and the existence of an optimal solution is established. Simulations are conducted for single, dual and triple control measures. The research shows that the time to reach the control target is the shortest when the three control measures are considered comprehensively. If only the vaccination rate or the vaccine protection level is increased separately, it will not control the spread of the disease effectively, even will cause a secondary outbreak of the disease or an endemic state.

The model established in this paper is based on simple assumptions of homogeneous population mixing and spatiotemporal invariance, without considering realistic factors such as population heterogeneity and spatial distribution. Additionally, we construct Bang-Bang control is a piecewise continuous strategy under unconstrained conditions, without accounting for practical considerations such as intervention costs, resource limitations, and random disturbances.In the future, we will conduct research from aspects such as age and spatial heterogeneity, and perform simulation studies using actual case data. Additionally, we will construct an optimal control framework with resource constraints, cost-effectiveness, and random disturbances to quantify the return on investment of prevention and control measures, providing more specific and reliable theoretical support for infectious disease prevention and control decisions.

Declaration of competing interest

The authors declare that they have no known competing financial interests or personal relationships that could have appeared to influence the work reported in this paper.

Acknowledgments

We would like to thank the reviewers for their valuable comments and suggestions which helped us to improve the presentation of this paper significantly.

CRediT authorship contribution statement

Ya Chen: Data curation, Formal analysis, Validation,Writing – original draft, Writing – review & editing. **Wenjun Jing**: Data curation, Formal analysis, Visualization, Writing – original draft, Writing – review & editing. **Juping Zhang**: Conceptualization, Investigation, Methodology, Supervision, Writing – review & editing. **Peng Qin**: Conceptualization, Data curation, Software, Supervision, Writing – review & editing.

Funding declaration

This work was supported by the National Natural Science Foundation of China (No.12471462, No.12101373, No.12171291), Fundamental Research Program of Shanxi Province (No.202403021211154).

Conflict of interest

Authors declare that they have no conflict of interest.

Data availability

All data generated or analysed during this study are included in this published article and

its supplementary information files.

References

[1] Centers for Disease Control and Prevention. COVID-19 Vaccination. 2022. https://www.cdc.gov/coronavirus/2019-ncov/vaccines/effectiveness/why-measure-effecti veness/breakthrough-cases.html

[2] Li Y, Qin S, Dong L, et al. Long-term effects of Omicron BA. 2 breakthrough infection on immunity-metabolism balance: a 6-month prospective study. Nature Communications. 2024, 15(1): 2444.

[3] Osterholm MT, Kelley NS, Sommer A, et al. Efficacy and effectiveness of influenza vaccines: a systematic review and meta-analysis. The Lancet Infectious Diseases. 2012, 12(1): 36-44.

[4] Gupta RK, Topol EJ. COVID-19 vaccine breakthrough infections. Science. 2021, 374(6575): 1561-1562.

[5] Centers for Disease Control and Prevention. Seasonal Influenza (Flu). 2021. https://www.cdc.gov/flu/professionals/antivirals/antiviral-use-influenza.htm

[6] Centers for Disease Control and Prevention. Chickenpox (Varicella). 2017. https://web.archive.org/web/20170225050958/https://www.cdc.gov/chickenpox/hcp/clin ical-overview.html

[7] Bergwerk M, Gonen T, Lustig Y, et al. COVID-19 breakthrough infections in vaccinated health care workers. New England Journal of Medicine. 2021, 385(16): 1474-1484.

[8] Alcendor D J, Matthews-Juarez P, Smoot D, et al. Breakthrough COVID-19 infections in the US: implications for prolonging the pandemic. Vaccines. 2022, 10(5): 755.

[9] Abu-Raddad LJ, Chemaitelly H, Ayoub HH, et al. Relative infectiousness of SARS-CoV-2 vaccine breakthrough infections, reinfections, and primary infections. Nature Communications. 2022, 13(1): 532.

[10] Chemaitelly H, Ayoub HH, Tang P, et al. Addressing bias in the definition of SARS-CoV-2 reinfection: implications for underestimation. Frontiers in Medicine. 2024, 11: 1363045.

[11] Pulliam JRC, van Schalkwyk C, Govender N, et al. Increased risk of SARS-CoV-2 reinfection associated with emergence of Omicron in South Africa. Science. 2022, 376(6593): 4947.

[12] Fonville J M, Wilks SH, James SL, et al. Antibody landscapes after influenza virus infection or vaccination. Science. 2014, 346(6212): 996-1000.

[13] Van der Kuyl A C, Cornelissen M. Identifying HIV-1 dual infections. Retrovirology. 2007, 4: 1-12.

[14] Ghosh M, Olaniyi S, Obabiyi OS. Mathematical analysis of reinfection and relapse in malaria dynamics. Applied Mathematics and Computation. 2020, 373: 125044.

[15] Anggriani N, Tasman H, Ndii MZ, et al. The effect of reinfection with the same serotype on dengue transmission dynamics. Applied Mathematics and Computation. 2019. 349: 62-80.

[16] Wang J, Kaperak C, Sato T, et al. COVID-19 reinfection: a rapid systematic review of case reports and case series. Journal of Investigative Medicine. 2021, 69(6): 1253-1255.

[17] Glynn J R, Murray J, Bester A, et al. High rates of recurrence in HIV-infected and HIV-uninfected patients with tuberculosis. The Journal of Infectious Diseases. 2010, 201(5): 704-711.

[18] Costenaro P, Minotti C, Barbieri E, et al. SARS-CoV-2 infection in people living with HIV: a systematic review. Reviews in Medical Virology. 2021, 31(1): 1-12.

[19] Mary K. People with HIV at higher risk of COVID reinfection: CDC. 2023. https://abcnews.go.com/Health/people-hiv-higher-risk-covid-reinfection-cdc/story?id=104035803

[20] Centers for Disease Control and Prevention. What is COVID-19 Reinfection? 2019. https://www.cdc.gov/coronavirus/2019-ncov/your-health/reinfection.html

[21] Perkins TA, Reiner RC JR, España G, et al. An agent-based model of dengue virus transmission shows how uncertainty about breakthrough infections influences vaccination impact projections. Plos Computational Biology. 2019, 15(3): e1006710.

[22] Azimaqin N, Peng Z, Ren X, et al. Vaccine failure, seasonality and demographic changes associate with mumps outbreaks in Jiangsu Province, China: Age-structured mathematical modelling study. Journal of Theoretical Biology. 2022, 544: 111125.

[23] Xu C, Wang Y, Cheng K, et al. A Mathematical Model to Study the Potential Hepatitis B Virus Infections and Effects of Vaccination Strategies in China. Vaccines. 2023, 11(10): 1530.

[24] Elbasha EH, Podder CN, Gumel AB. Analyzing the dynamics of an SIRS vaccination model with waning natural and vaccine-induced immunity. Nonlinear Analysis: Real World Applications. 2011, 12(5): 2692-2705.

[25] Yuliana R, Alfiniyah C, Windarto W. Stability analysis of SIVS epidemic model with vaccine ineffectiveness. AIP Conference Proceedings. 2021, 2329(1).

[26] Jing S, Xue L, Li X, et al. Age-structured modeling of COVID-19 dynamics: the role of treatment and vaccination in controlling the pandemic. Journal of Mathematical Biology. 2025, 90(1): 1-49.

[27] Montalbán A, Corder RM, Gomes MGM. Herd immunity under individual variation and reinfection. Journal of Mathematical Biology. 2022, 85(1): 2.

[28] Rehman A, Singh R, Singh J. Mathematical analysis of multi-compartmental malaria transmission model with reinfection. Chaos, Solitons & Fractals. 2022,163: 112527.

[29] Anggriani N, Tasman H, Ndii M Z, et al. The effect of reinfection with the same serotype on dengue transmission dynamics. Applied Mathematics and Computation. 2019, 349: 62-80.

[30] Gomes MGM, White LJ, Medley G F. Infection, reinfection, and vaccination under suboptimal immune protection: epidemiological perspectives. Journal of Theoretical Biology. 2004, 228(4): 539-549.

[31] Agusto F B. Mathematical model of Ebola transmission dynamics with relapse and reinfection. Mathematical Biosciences. 2017, 283: 48-59.

[32] Rodrigues P, Margheri A, Rebelo C, Gomes MG. Heterogeneity in susceptibility to infection can explain high reinfection rates. Journal of Theoretical Biology. 2009, 259(2): 280-290.

[33] Megala T, Nandha Gopal T, Siva Pradeep M, et al. Dynamics of re-infection in a Hepatitis B Virus epidemic model with constant vaccination and preventive measures. Journal of Applied Mathematics and Computing. 2025: 1-27.

[34] Van den Driessche P. Reproduction numbers of infectious disease models. Infectious Disease Modelling. 2017, 2(3): 288-303.

[35] Fleming WH, Rishel RW. Deterministic and Stochastic Optimal Control. Springer-Verlag, New York. 1975.

[36] Pontryagin LS. Mathematical Theory of Optimal Processes. CRC Press. 1987.

Appendix

The proof of Lemma 1

Proof Summing the four equations of system (1) up yields $\frac{dN}{dt} = 0$. Thus the total population $N(t)$ is a constant. For convenience, let $N(t) = K$. Next, we prove that the solution of system (1) is non-negative.

Solving to the third equation of system (1) yields

$$I(t) = I(0)e^{-\int_0^t (-\frac{(S(x)+\sigma V(x)+\epsilon R(x))\beta}{N}+\eta)dx} \geq 0.$$

Plugging it into the fourth equation of system (1), we can get

$$R(t) = R(0) + \int_0^t e^{\int_0^x (\frac{\beta\epsilon I(y)}{N}+\gamma)dy} \eta I(x)dx \; e^{-\int_0^t (\frac{\beta\epsilon I(x)}{N}+\gamma)dx} \geq 0,$$

Besides, sloving the first equation of system (1), we obtion

$$S(t) = S(0) + \int_0^t \left(e^{\int_0^x (\frac{\beta I(y)}{N}+\alpha)dy} (\theta V(x) + \gamma R(x)) \right) dx \; e^{-\int_0^t (\frac{\beta I(x)}{N}+\alpha)dx},$$

Let $t_1 > 0$ be the first time that $\min\{S(t_1), V(t_1)\} = 0$. Assuming that $S(t_1) = 0$, then $S(t)$ and $V(t) > 0$, for $\forall t \in [0, t_1)$. Furthermore we can get

$$S(t_1) = S(0) + \int_0^{t_1} \left(e^{\int_0^x (\frac{\beta I(y)}{N}+\alpha)dy} (\theta V(x) + \gamma R(x)) \right) dx \; e^{-\int_0^t (\frac{\beta I(x)}{N}+\alpha)dx} > 0,$$

this contradicts the assumption $S(t_1) = 0$. Similarly, let us assume that $V(t_1) = 0$, then according to the second equation of system (1), we can get

$$V(t_1) = V(0) + \int_0^{t_1} \left(e^{\int_0^x (\frac{\sigma\beta I}{N}+\theta)dx} \alpha S(x) \right) dx \; e^{-\int_0^t (\frac{\sigma\beta I}{N}+\theta)dx} > 0,$$

which contradicts the assumption of $V(t_1) = 0$. This mean that all solution of system (1) are non-negative and Γ is the positively invariant set of system (1). This completes the proof.

The proof of Theorem 1

Proof The Jacobian matrix of system (2) at the disease-free equilibrium P_0 is

$$K(P_0) = \begin{bmatrix} -\alpha-\gamma & \theta-\gamma & -\frac{\beta\theta}{\alpha+\theta}-\gamma \\ \alpha & -\theta & -\frac{\sigma\beta\alpha}{\alpha+\theta} \\ 0 & 0 & \frac{\beta(\sigma\alpha+\theta)}{\alpha+\theta}-\eta \end{bmatrix}.$$

The characteristic polynomial corresponding to matrix $K(P_0)$ is

$$\lambda^3 + a_2\lambda^2 + a_1\lambda + a_0 = 0, \tag{a}$$

where

$$a_2 = \frac{\alpha^2 + (-\sigma\beta + \eta + \gamma + 2\theta)\alpha + \theta(\eta - \beta + \gamma + \theta)}{\alpha + \theta}, \tag{b}$$

$$a_1 = \frac{\alpha^2(-\sigma\beta + \eta + \gamma) + \alpha[\theta(2\gamma - (\sigma+1)\beta + 2\eta) + \gamma(-\sigma\beta + \eta)] + \theta[(\eta - \beta + \gamma)\theta + \gamma(\eta - \beta)]}{\alpha + \theta}, \tag{c}$$

$$a_0 = \gamma[(-\sigma\beta + \eta)\alpha + \theta(\eta - \beta)]. \tag{d}$$

The roots of the characteristic polynomial (a) are $\lambda_1 = -\gamma$, $\lambda_2 = -\alpha - \theta$, $\lambda_3 = \frac{\beta(\sigma\alpha+\theta)-\eta(\alpha+\theta)}{\alpha+\theta}$. Obviously, when $R_0 < 1$, $\lambda_3 < 0$. Therefore, the disease-free equilibrium P_0 of system (2) is locally asymptotically stable, if $R_0 < 1$.

When $R_0 = 1$, $\lambda_3 = 0$. At this time, the central manifold theorem is used to prove the stability of the disease-free equilibrium P_0. The following affine transformation is defined

$$\begin{bmatrix} s \\ v \\ i \end{bmatrix} = \begin{bmatrix} \frac{\theta}{\alpha+\theta} \\ \frac{\alpha}{\alpha+\theta} \\ 0 \end{bmatrix} + \begin{bmatrix} \frac{\theta-\gamma}{\alpha} & -1 & \frac{(-\eta-\gamma)\theta^2-\sigma(\eta+\gamma)\alpha\theta+\alpha\eta\gamma\sigma}{(\alpha+\theta)(\alpha\sigma+\theta)\gamma} \\ 1 & 1 & -\frac{\alpha[(\eta+\gamma)\sigma\alpha+(\eta\sigma+\theta)\gamma+\theta\eta]}{(\alpha+\theta)(\alpha\sigma+\theta)\gamma} \\ 0 & 0 & 1 \end{bmatrix} \begin{bmatrix} \bar{s} \\ \bar{v} \\ \bar{i} \end{bmatrix}. \tag{e}$$

Furthermore,

$$\begin{aligned} \frac{d\bar{s}}{dt} &= -\gamma\bar{s} + G_{11}\bar{s}\bar{i} + G_{12}\bar{v}\bar{i} + O(|\bar{s},\bar{v},\bar{i}|^2), \\ \frac{d\bar{v}}{dt} &= -(\alpha+\theta)\bar{v} + G_{21}\bar{s}\bar{i} + G_{22}\bar{v}\bar{i} + O(|\bar{s},\bar{v},\bar{i}|^2) \\ \frac{d\bar{i}}{dt} &= \frac{(1-R_*)\eta(\alpha+\theta)(\alpha\sigma+\theta)\epsilon}{(\alpha\sigma+\theta)^2\gamma}\bar{i}^2 + G_{31}\bar{s}\bar{i} + G_{32}\bar{v}\bar{i}, \end{aligned} \tag{f}$$

the linear part here is the Jordan canonical form of the matrix K, and

$$G_{11} = \frac{\{[(\sigma-\epsilon)\eta - \gamma\epsilon]\alpha + [(\epsilon-1)\eta + \gamma\epsilon](\gamma-\theta)\}(\alpha+\theta)\eta}{(\alpha\sigma+\theta)\gamma(\alpha-\gamma+\theta)}, G_{12} = \frac{(\sigma-1)(\alpha+\theta)\alpha\eta^2}{(\alpha\sigma+\theta)\gamma(\alpha-\gamma+\theta)},$$

$$G_{21} = \frac{-\eta}{(\alpha-\gamma+\theta)(\alpha\sigma+\theta)^2}\{(\sigma-1)\theta^3 + [\alpha\sigma^2 + ((\epsilon-1)\eta-\gamma)\sigma + (2-\epsilon)\gamma - \alpha + (1-\epsilon)\eta]\theta^2$$
$$+[-\alpha(\eta-\alpha+\gamma)\sigma^2 + (((2-\epsilon)\alpha - 2(\epsilon-1)\eta)\gamma + \alpha(-\alpha+\eta(\epsilon+1)))\sigma + (\epsilon-1)\gamma^2$$
$$+(\epsilon-1)(\eta-\alpha)\gamma - \alpha\eta\epsilon]\theta + \sigma\gamma(\eta\alpha\sigma + (\epsilon-1)(\eta+\alpha)\gamma + (1-\epsilon)\alpha^2 - \alpha\eta\epsilon)\gamma^r,$$

$$G_{22} = \frac{-\eta}{(\alpha-\gamma+\theta)(\alpha\sigma+\theta)^2}\{\sigma\alpha^3 + [(\sigma^2+\sigma+1)\theta - \gamma\sigma]\alpha^2 + [(\sigma^2+\sigma+1)\theta^2 + ((-\eta-\gamma)\sigma^2 + 2\eta\sigma - \eta - \gamma)\theta + \eta\gamma\sigma(\sigma-1)]\alpha - \theta^2\sigma(\gamma-\theta)\},$$

$$G_{31} = \frac{(\alpha+\theta)[(\sigma-\epsilon)\alpha + (\epsilon-1)(\gamma-\theta)]\eta}{\alpha(\alpha\sigma+\theta)}, G_{32} = \frac{(\sigma-1)(\alpha+\theta)\eta}{\alpha\sigma+\theta}.$$

Let $R_* = \frac{[(\alpha\sigma+\theta)(\gamma+\eta)+\gamma\eta\sigma](\alpha\sigma+\theta)}{\eta(\alpha+\theta)[(\alpha\sigma+\theta)\epsilon+\gamma\sigma]}$. Then, if $R_0 /= R_*$,there exists a one-dimensional central manifold

$$\bar{s} = \frac{\eta^2\alpha\{\eta(1-R_*)(\alpha+\theta)[(\alpha\sigma+\theta)\epsilon+\gamma\sigma] + \gamma\theta\epsilon(\alpha\sigma+\alpha+\theta)\}}{(\alpha-\gamma+\theta)(\alpha\sigma+\theta)^2\gamma^3}\bar{i}^2 + O(|\bar{i}|^3),$$

$$\bar{v} = \frac{[\theta(\sigma-1)(\alpha+\theta-\gamma) + \eta\theta(1-\sigma) + \gamma\eta\sigma](R_*-1)[(\alpha+\theta)\sigma+\gamma\sigma]}{(\alpha\sigma+\theta)^3(\alpha+\theta)(\alpha+\theta-\gamma)\gamma} + \frac{\eta\sigma^2}{(\alpha\sigma+\theta)^3}\bar{i}^2 + \frac{\eta\epsilon(\sigma\theta-\gamma\sigma-\theta)}{(\alpha\sigma+\theta)^2(\alpha+\theta-\gamma)}\bar{i}^2 + O(|\bar{i}|^3),$$

Therefore, system (2) is simplified to

$$\frac{d\bar{i}}{dt} = -\frac{\eta[(\eta+\gamma)(\alpha\sigma+\theta)^2 + \eta\alpha\gamma(\sigma^2-\sigma) - \eta(\alpha+\theta)(\alpha\sigma+\theta)\epsilon]}{(\alpha\sigma+\theta)^2\gamma}\bar{i}^2 + O(|\bar{i}|^3) = \frac{\eta^2(1-R_*)(\alpha+\theta)[(\alpha\sigma+\theta)\epsilon+\gamma\sigma]}{(\alpha\sigma+\theta)^2\gamma}\bar{i}^2 + O(|\bar{i}|^3).$$

It is to see that disease-free equilibrium P_0 is a saddle node. When $R_0 = R_*$, according to the center manifold theorem, the center manifold of system (2) at the far point can be expressed as

$$\frac{d\bar{i}}{dt} = -\frac{\eta}{\gamma(\alpha\sigma+\theta)^4}\{[\eta(\alpha+\theta)(\alpha\sigma+\theta)\epsilon + \eta\gamma\sigma^2\alpha](\alpha\sigma+\theta)^2 + \gamma\alpha\eta^2\sigma^2(1-\sigma)(\alpha+\theta)\}\bar{i}^3 + O(|\bar{i}|^4).$$

Since $\sigma, \epsilon \in [0,1]$, the disease-free equilibrium P_0 is a stable node, when $R_0 = 1$ and $R_0 = R_*$.

The proof of Theorem 2

Proof The Jacobian matrix of system (2) at the equilibrium P_2 is

$$K(P_2) = \begin{bmatrix} -\beta i_2 & -\alpha-\gamma & \theta-\gamma & -\frac{\beta(\beta i_2\sigma+\theta)\gamma(1-i_2)}{\beta^2 i_2^2\sigma+\beta(\alpha\sigma+\gamma\sigma+\theta)i_2+\gamma(\alpha+\theta)} - \gamma \\ \beta i_2 & \alpha & -\sigma\beta i_2-\theta & -\frac{\beta\sigma\alpha\gamma(1-i_2)}{\beta^2 i_2^2\sigma+\beta(\alpha\sigma+\gamma\sigma+\theta)i_2+\gamma(\alpha+\theta)} \\ 0 & \beta(1-\epsilon)i_2 & \beta(\sigma-\epsilon)i_2 & \frac{\beta[(1-\epsilon)(\beta i_2\sigma+\theta)+(\sigma-\epsilon)\alpha]\gamma(1-i_2)}{\beta^2 i_2^2\sigma+\beta(\alpha\sigma+\gamma\sigma+\theta)i_2+\gamma(\alpha+\theta)} + \beta\epsilon(1-2i_2) - \eta \end{bmatrix}.$$

The characteristic equation of $K(P_2)$ is

$$\Lambda^3 + d_2\Lambda^2 + d_1\Lambda + d_0 = 0, \quad (g)$$

where

$$d_2 = \frac{1}{h}\{b_3 i_2^3 + \beta^3\sigma i_2^3(\sigma+1) + \beta^2 i_2^2(\sigma^2\alpha + \gamma\sigma\epsilon + \sigma^2\gamma + 2\gamma\sigma + \theta) + 2\beta^2 i_2^2\sigma(\alpha+\theta) + \beta^2 i_2^2\epsilon(\alpha\sigma+\theta) + \gamma\beta i_2(\alpha\sigma+\theta) + i_2\beta[\alpha\sigma + \theta + \gamma(2\sigma+\epsilon+1)](\alpha+\theta) + \beta\gamma^2\sigma i_2 + \gamma(\alpha+\theta)(\alpha+\gamma+\theta) + f(i_2),$$

$$d_1 = \frac{1}{h}\{[(1+\sigma)b_3 + \beta^3\sigma^2]\beta i_2^4 + \beta^2 i_2^3[(\epsilon+2)(\alpha+\gamma)\sigma^2 + (2\alpha+\gamma+2\theta)\epsilon\sigma + (2\sigma+\epsilon)\theta] + \beta^2 i_2^2[\epsilon(\alpha+\theta)(\alpha\sigma+2\gamma\sigma+\gamma+\theta) + \theta^2 + 2\sigma(\alpha+2\gamma)\theta + 3\alpha\gamma\sigma + (\alpha^2+\alpha\gamma+\gamma^2)\sigma^2 + \gamma\sigma\beta(1-\epsilon)] + \beta i_2\gamma[\beta\theta(1-\epsilon) - \alpha\beta\epsilon\sigma + \alpha\beta\sigma^2 + \alpha^2\epsilon + 2\alpha^2\sigma + 2\alpha\epsilon\theta + 2\alpha\gamma\sigma + 2\alpha\sigma\theta + \theta^2\epsilon + 2\gamma\sigma\theta + \alpha\gamma + 2\alpha\theta + \gamma\theta + 2\theta^2] + \gamma^2(\alpha+\theta)^2,$$

$$d_0 = \frac{1}{h}((\alpha\gamma + \gamma\theta - \beta^2\sigma i_2)^2 f(i_2) + (\beta\theta i_2^2 + \alpha\gamma i_2 + \gamma\theta i_2 + \beta\gamma\sigma i_2^2 + \alpha\beta\sigma i_2^2 + \beta^2\sigma i_2^3)g(i_2)),$$

$$h_2 = \beta^2 i_2^2\sigma + \beta(\alpha\sigma + \gamma\sigma + \theta)i_2 + \gamma(\alpha+\theta).$$

Obviously, $d_2 > 0$, $f(i_2) = 0$. According to $R_0 < 1$ and $R_* < R_0$, we have that $g(i_2) < 0$, $d_0 < 0$. Let the three roots of equation (g) be Λ_1, Λ_2 and Λ_3, respectively. According to Vieta's theorem, it has

$$\Lambda_1\Lambda_2\Lambda_3 = -d_0 > 0, \tag{h}$$

$$\Lambda_1 + \Lambda_2 + \Lambda_3 = -d_2 < 0. \tag{i}$$

Therefore, according to expression (h), the roots of equation (g) include the following three cases: three positive roots, one positive root and a pair of conjugate complex roots, one positive root and two negative roots. According to expression (i), equation (g) has a pair of conjugate complex roots or negative roots with negative real parts. In summary, there are two cases of the roots of equation (g): one positive root and a pair of conjugate complex roots, one positive root and two negative roots. Therefore, the endemic equilibrium P_2 is unstable.

The proof of Theorem 3

Proof The Jacobian matrix of system (2) at the endemic equilibrium P_3 is

$$K(P_3) = \begin{bmatrix} -\beta i_3 - \alpha - \gamma & \theta - \gamma & -\frac{\gamma[\gamma(\alpha+\theta)+\beta\theta]}{\beta\theta i_3 + \gamma(\alpha+\theta)} \\ \alpha & -\theta & 0 \\ \beta(1-\epsilon)i_3 & -\beta\epsilon i_3 & \frac{-2\beta^2\epsilon\theta i_3^2 - [(\gamma-\beta)\epsilon\theta + (\eta+\gamma)\theta + \alpha\gamma\epsilon]\beta i_3 - \gamma[\alpha\eta + (\eta-\beta)\theta]}{(\beta i_3+\gamma)\theta + \alpha\gamma} \end{bmatrix},$$

The characteristic equation of $K(P_3)$ is

$$\Lambda^3 + e_2\Lambda^2 + e_1\Lambda + e_0 = 0, \tag{j}$$

where

$$e_2 = \frac{1}{h_3}\{\beta^2\theta i_3^2(1+\epsilon) + \beta i_3[(\epsilon+2)\theta\gamma + \alpha(1+\epsilon)\gamma + \theta(\alpha+\theta)] + \gamma(\alpha+\theta)(\alpha+\gamma+\theta) + F(i_3),$$

$$e_1 = \frac{1}{h_3}\{\beta^2 i_3^2[(\alpha\gamma+\alpha\theta+\theta^2)\epsilon+\theta^2] + \beta\gamma i_3[\alpha^2\epsilon + 2(1+\epsilon)\theta\alpha + (\eta+\gamma)\alpha + \theta^2(2+\epsilon)] + \gamma^2(\alpha+\theta)^2 + (\alpha+\gamma+\theta)F(i_3) + (\beta i_3^2 + \gamma\beta_3)G(i_3),$$

$$e_0 = \frac{1}{h_3}[(\alpha\gamma+\gamma\theta)^2 F(i_3) + (\beta\theta i_2^2 + \alpha\gamma i_3 + \gamma\theta i_3)G(i_3)], h_3 = \beta\theta i_3^2 + \gamma(\alpha+\theta).$$

Obviously, $e_2 > 0$, $e_1 > 0$, $F(i_3) = 0$. According to $R_{**} < R_0$, $R_* < R_0$ and $R_* < 1$, we obtain that $G(i_3) > 0$, and then $e_0 > 0$. Therefore,

$$H_1 = e_2 > 0,$$

$$\begin{aligned}
H_2 &= \begin{vmatrix} 1 & e_0 \\ 1 & e_1 \end{vmatrix} = \\
&= (2\alpha\beta^4\epsilon^2\gamma\theta + \alpha\beta^4\epsilon^2\theta^2 + \beta^4\epsilon^2\theta^3 + \alpha\beta^4\epsilon\gamma\theta + \alpha\beta^4\epsilon\theta^2 + 3\alpha\beta^3\epsilon^2\gamma^2\theta + 4\alpha\beta^3\epsilon^2\gamma\theta^2 \\
&\quad + 2\beta^4\epsilon\theta^3 + \beta^4\theta^3)i_3^4 + [2\gamma^2\alpha\beta^3\epsilon\theta(1-\epsilon) + \alpha^2\beta^3\epsilon^2\gamma^2 + 2\alpha^2\beta^3\epsilon^2\gamma\theta + 2\beta^3\epsilon^2\gamma\theta^3 \\
&\quad + \alpha^2\beta^3\epsilon\gamma^2 + 3\alpha^2\beta^3\epsilon\gamma\theta + \alpha^2\beta^3\epsilon\theta^2 + \alpha\beta^3\eta\gamma\theta + 4\alpha\beta^3\epsilon\gamma^2\theta + 9\alpha\beta^3\epsilon\gamma\theta^2 + 2\alpha\beta^3\epsilon\theta^3 \\
&\quad + 6\beta^3\epsilon\gamma\theta^3 + \beta^3\epsilon\theta^4 + \alpha\beta^3\eta\gamma\theta + \alpha\beta^3\gamma^2\theta + 3\alpha\beta^3\gamma\theta^2 + \alpha\beta^3\theta^3 + 4\beta^3\gamma\theta^3 + \beta^3\theta^4]i_3^3 \\
&\quad + (\alpha^3\beta^2\epsilon^2\gamma^2 + 3\alpha^2\beta^2\epsilon^2\gamma^2\theta + 3\alpha\beta^2\epsilon^2\gamma^2\theta^2 + \beta^2\epsilon^2\gamma^2\theta^3 + 2\alpha^3\beta^2\epsilon\gamma^2 + 2\alpha^3\beta^2\epsilon\gamma\theta \\
&\quad + 2\alpha^2\beta^2\epsilon\gamma^3 + 10\alpha^2\beta^2\epsilon\gamma^2\theta + 6\alpha^2\beta^2\epsilon\gamma\theta^2 + 2\alpha\beta^2\epsilon\gamma^3\theta + 14\alpha\beta^2\epsilon\gamma^2\theta^2 + 6\alpha\beta^2\epsilon\gamma\theta^3 \\
&\quad + 6\beta^2\epsilon\gamma^2\theta^3 + 2\beta^2\epsilon\gamma\theta^4\alpha^2\beta^2\eta\gamma^2 + \alpha^2\beta^2\eta\gamma\theta + \alpha^2\beta^2\gamma^3 + 4\alpha^2\beta^2\gamma^2\theta + 3\alpha^2\beta^2\gamma\theta^2 \\
&\quad + 3\alpha\beta^2\eta\gamma^2\theta + \alpha\beta^2\eta\gamma\theta^2 + 2\alpha\beta^2\gamma^3\theta + 10\alpha\beta^2\gamma^2\theta^2 + 6\alpha\beta^2\gamma\theta^3 + 6\beta^2\gamma^2\theta^3 + 3\beta^2\gamma\theta^4)i_3^2 \\
&\quad + (\alpha^2\beta\epsilon\gamma^2 + 2\alpha^3\beta\epsilon\gamma^3 + 4\alpha^3\beta\epsilon\gamma^2\theta + 6\alpha^2\beta\epsilon\gamma^3\theta + 6\alpha^2\beta\epsilon\gamma^2\theta^2 + \alpha\beta^2\gamma^3\theta + 6\alpha\beta\epsilon\gamma^3\theta^2 \\
&\quad + 4\alpha\beta\epsilon\gamma^2\theta^3 + 2\beta\epsilon\gamma^3\theta^3 + \beta\epsilon\gamma^2\theta^4 + \alpha^3\beta\eta\gamma^2 + 2\alpha^3\beta\gamma^3 + 3\alpha^3\beta\gamma^2\theta + 2\alpha^2\beta\eta\gamma^2\theta \\
&\quad + \alpha^2\beta\gamma^4 + 8\alpha^2\beta\gamma^3\theta + 9\alpha^2\beta\gamma^2\theta^2 + \alpha\beta^2\gamma^3\theta + \alpha\beta\eta\gamma^2\theta^2 + \alpha\beta\gamma^4\theta + 10\alpha\beta\gamma^3\theta^2 \\
&\quad + 9\alpha\beta\gamma^2\theta^3)i_3 + 4\beta\gamma^3\theta^3 + 3\beta\gamma^2\theta^4 + \gamma^3(\alpha+\theta)^3(\alpha+\gamma+\theta) + (\beta i_3\epsilon + \gamma)\alpha\gamma\beta i_3 f(i_3) \\
&\quad + [\beta^3\theta(\epsilon+1)i_3^4 + \beta^2(2\epsilon\theta\gamma + 3\theta\gamma + \alpha\gamma + \alpha^2 + \alpha\theta)i_3^3 + (\epsilon\theta\gamma + 3\theta\gamma + \alpha\epsilon\gamma + \alpha^2 \\
&\quad + \alpha\theta)\beta\gamma i_3^2 + (\alpha+\theta)i_3]g(i_3) > 0,
\end{aligned}$$

$$H_3 = \begin{vmatrix} 1 & e_2 & e_0 & 0 \\ 1 & 1 & e_1 & 0 \\ 0 & e_2 & e_0 & \end{vmatrix} = e_0 H_2 > 0.$$

According to the Hurwitz criterion, all the roots of equation (j) have negative real parts. Therefore, the endemic equilibrium P_3 is locally asymptotically stable.

The proof of Lemma 2

Proof Let

$$\vec{f}_*(t,\vec{x}) = \begin{bmatrix} -\beta si + \theta v + \gamma(1-s-v-i) \\ -\sigma\beta vi - \theta v \\ \beta\left[s + \sigma v + \epsilon(1-s-v-i)\right] i - \eta i \end{bmatrix},$$

$$\vec{g}_*(t,\vec{x},\vec{u}) = \begin{bmatrix} \beta si & -s & 0 \\ (1-u_3)\sigma\beta vi & s & (1-u_1)\sigma\beta vi \\ -\beta\left[s + (1-u_3)\sigma v + \epsilon(1-s-v-i)\right] i & 0 & -(1-u_1)\beta\sigma vi \end{bmatrix}$$

Then, system (7) can be rewritten as $\vec{x}'(t) = \vec{f}_*(t,\vec{x}) + \vec{g}_*(t,\vec{x},\vec{u})\vec{u}$. We prove that the following four conditions are satisfied:

(i) $\vec{f}_*(t,\vec{x}) + \vec{g}_*(t,\vec{x},\vec{u})u$ is first-order continuously differentiable, and there exists a constant C such that

$$|\vec{f}_*(t,0,0)| \le C, |\vec{f}_*(\vec{x}) + \vec{g}_*(\vec{x},\vec{u})\vec{u}| \le C(1+|\vec{u}|), |\vec{g}_*(\vec{x},\vec{u})| \le C.$$

(ii) The solution set of system (7) corresponding to the control parameters in the control set U is non-empty.

(iii) The dominating set U is a closed convex compact set.

(iv) The integrand in the objective function J is convex in U.

Firstly, it is easy to see that $\vec{f}_*(t,\vec{x}) + \vec{g}_*(t,\vec{x},\vec{u})u$ is first-order continuously differentiable, and $|\vec{f}_*(t,0,0)| = 0$. Since s, v, i are non-negative and bounded, there exists a constant C such that $|\vec{f}_*(t,0,0)| \le C, |\vec{f}_*(\vec{x}) + \vec{g}_*(\vec{x},\vec{u})\vec{u}| \le C(1+|\vec{u}|), |\vec{g}_*(\vec{x},\vec{u})| \le C$. This shows that condition (i) is true, It can be seen that the system (7) has a unique solution, which means that condition (ii) is established.

The control set U is a closed convex compact set and the integrand of the objective function is a constant function. So conditions (iii) and (iv) are valid. In summary, the time optimal control problem has an optimal solution.

The proof of Theorem 4

Proof In order to find the minimum disease eradication time and the time-dependent control variable $\vec{u}^*(t)$, it is equivalent to the problem of minimizing the Hamiltonian system. Let the

Hamiltonian system be

$$\begin{aligned} H(\vec{x}, \Lambda_1, \Lambda_2, \Lambda_3, t) &= 1 + \Lambda_1 \frac{ds}{dt} + \Lambda_2 \frac{dv}{dt} + \Lambda_3(t) \frac{di}{dt} \\ &= 1 + \Lambda_1(t)\left[-(1-u_1)\beta si - u_2 s + \theta v + \gamma(1-s-v-i)\right] \\ &\quad + \Lambda_2(t)\left[-(1-u_1)(1-u_3)\sigma\beta vi - \theta v + u_2 s\right] \\ &\quad + \Lambda_3(t)\left\{(1-u_1)\beta\left[s + (1-u_3)\sigma v + \epsilon(1-s-v-i)\right] i - \eta i\right\}, \end{aligned} \tag{k}$$

where Λ_1, Λ_2, Λ_3 are the adjoint variables associated with the state variables s, v, i. Using the Pontryagin maximum principle [36], we can see that the relationship between adjoint control and optimal control is as follows

$$\frac{d\Lambda_1}{dt} = -\frac{\partial H}{\partial s}, \frac{d\Lambda_2}{dt} = -\frac{\partial H}{\partial v}, \frac{d\Lambda_3}{dt} = -\frac{\partial H}{\partial i}, \tag{l}$$

and the transversality condition is $\Lambda_1(T) = \Lambda_2(T) = \Lambda_3(T) = 0$.

Therefore, the adjoint system is

$$\begin{aligned} \frac{d\Lambda_1}{dt} &= \Lambda_1\left[(1-u_1)\beta i + u_2 + \gamma\right] - \Lambda_2 u_2 + \Lambda_3(1-u_1)\beta(-1+\epsilon)i, \\ \frac{d\Lambda_2}{dt} &= \Lambda_1(-\theta+\gamma) + \Lambda_2(t)\left[(1-u_1)(1-u_3)\sigma\beta i + \theta\right] + \Lambda_3(1-u_1)\beta\left[-(1-u_3)\sigma + \epsilon\right] i, \\ \frac{d\Lambda_3}{dt} &= \Lambda_1(t)\left[(1-u_1)\beta s + \gamma\right] + \Lambda_2(1-u_1)(1-u_3)\sigma\beta v - \Lambda_3(1-u_1)\beta[s + (1-u_3)\sigma v \\ &\quad + \epsilon(1-s-v-2i)]i + \Lambda_3\eta. \end{aligned} \tag{m}$$

The corresponding switching functions and their time derivatives are

$$\Phi(\vec{x}, \Lambda_1, \Lambda_2, \Lambda_3, t) = \begin{bmatrix} (\Lambda_1 - \Lambda_3)\beta si + (\Lambda_2 - \Lambda_3)(1-u_3)\sigma\beta vi + \Lambda_3\beta\epsilon(1-s-v-i)i \\ (\Lambda_2 - \Lambda_1)s \\ (\Lambda_2 - \Lambda_3)(1-u_1)\sigma\beta vi \end{bmatrix}, \tag{n}$$

$$\frac{d\Phi}{dt}(\vec{x}, \Lambda_1, \Lambda_2, \Lambda_3, t) = \begin{bmatrix} \phi_1 \\ (\Lambda_2 - \Lambda_1)\frac{ds}{dt} + \left(\frac{d\Lambda_2}{dt} - \frac{d\Lambda_1}{dt}\right)s \\ \phi_3 \end{bmatrix}, \tag{o}$$

where

$$\begin{aligned} \phi_1 &= \left(\frac{d\Lambda_1}{dt} - \frac{d\Lambda_3}{dt}\right)\beta si + (\Lambda_1 - \Lambda_3)\beta\left(\frac{ds}{dt}i + \frac{di}{dt}s\right) + \left(\frac{d\Lambda_2}{dt} - \frac{d\Lambda_3}{dt}\right)(1-u_3)\sigma\beta vi + (\Lambda_2 - \Lambda_3)\left(1 - \frac{du_3}{dt}\right)\sigma\beta vi \\ &\quad + (\Lambda_2 - \Lambda_3)(1-u_3)\sigma\beta\left(\frac{dv}{dt}i + v\frac{di}{dt}\right) + \frac{d\Lambda_3}{dt}\beta\epsilon(1-s-v-i)i \\ &\quad + \Lambda_3\beta\epsilon(1-s-v-i)\frac{di}{dt} - \Lambda_3\beta\epsilon\left(\frac{ds}{dt} + \frac{dv}{dt} + \frac{di}{dt}\right)i, \\ \phi_3 &= \left(\frac{d\Lambda_2}{dt} - \frac{d\Lambda_3}{dt}\right)(1-u_3)\sigma\beta vi + (\Lambda_2 - \Lambda_3)\left(1 - \frac{du_1}{dt}\right)\sigma\beta vi + (\Lambda_2 - \Lambda_3)(1-u_3)\sigma \end{aligned}$$

$$\beta\left(\frac{dv}{dt}i + v\frac{di}{dt}\right),$$

Next, we prove that the switching function Φ disappears only at isolated points. Assuming that $\Phi(\vec{x}, \Lambda_1, \Lambda_2, \Lambda_3, t)$ disappears in an open set L, then in the neighborhood L, $\Phi = \frac{d\Phi}{dt} = 0$, so there is $\Lambda_1 = \Lambda_2 = \Lambda_3 = 0$. Then, the Hamiltonian system calculated along the optimal solution can be $H(\vec{x}, \Lambda_1, \Lambda_2, \Lambda_3, t) = 1 = 0$, which creates a contradiction. This implies that $\vec{u}^*(t)$ is a Bang-Bang control, that is a piecewise function.